Alkali–Methanol–Anthraquinone Pulping of *Miscanthus x giganteus* for Thermoplastic Composite Reinforcement

L. Lundquist,[1,*] G. Arpin,[1] Y. Leterrier,[1] F. Berthold,[2] M. Lindström,[2] J.-A. E. Månson[1]

[1]*Laboratoire de Technologie des Composites et Polymères (LTC), Ecole Polytechnique Fédérale de Lausanne (EPFL), CH 1015 Lausanne, Switzerland*
[2]*Swedish Pulp and Paper Research Institute (STFI), Box 5604, SE 114 86 Stockholm, Sweden*

Received 14 April 2003; accepted 20 November 2003

ABSTRACT: The potential of pulp fiber–reinforced thermoplastics is currently not fully explored in composites. One of the main reasons is that pulp fibers are extracted for the use in papermaking and are thus not optimized for use as reinforcements in thermoplastics. Furthermore, currently used processing methods constitute several severe thermomechanical steps inducing premature degradation of the fibers. A systematic development of these composite materials requires the study of both these aspects. The goal of this work was to optimize fiber extraction against properties relevant to the reinforcement of thermoplastics. To this end, thick-walled *Miscanthus x giganteus* pulp fibers were selected. The fibers were pulped by the alkaline–methanol–anthraquinone process. An unreplicated factorial design was applied to determine the effect of key operating variables on fiber thermal stability and mechanical properties. The thermomechanical properties of pulp fibers depend primarily on the morphology and chemical composition of the fiber resource in terms of the respective amounts of lignin, hemicellulose, and cellulose, all strongly influenced by the choice of pulping conditions. Optimal pulping parameters were identified, allowing production of fibers thermally stable up to 255°C with an aspect ratio of 40, a straightness of 95%, and tensile strength as high as 890 MPa. Specific stiffness and strength values with respect to density and material cost of 56 GPa $m^{-3}\$^{-1}$ and 820 MPa m^{-3} $\$^{-1}$ were highly competitive with glass fibers, with corresponding values of 15 GPa $m^{-3}\$^{-1}$ and 270–490 MPa m^{-3} $\$^{-1}$, respectively. © 2004 Wiley Periodicals, Inc. J Appl Polym Sci 92: 2132–2143, 2004

Key words: alkali–methanol–anthraquinone pulping; delignification; thermal stability; zero-span tensile index; *Miscanthus x giganteus*

INTRODUCTION

Several authors have investigated the use of pulp fibers for reinforcement of thermoplastics as reviewed by Bledzki and Gassan.[1] However, common to a large majority of previous studies is that they rarely provide full information as to the source and properties of the used fibers. Descriptions such as "thermochemical pulp,"[2] "bleached kraft cellulose,"[3] and "hardwood high α-cellulose"[4] are found in the literature. Given the considerable property differences that are observed in terms of shape, size, and mechanical properties as a function of fiber source and pulping method and conditions, this information is in fact largely insufficient for a judgment of the reinforcement efficiency of a given fiber. This lack of attention to fibers' intrinsic properties is primarily attributed to two reasons.

First, the research community has long since been preoccupied with the problem of dispersion and compatibilization of hydrophilic pulp fibers with hydrophobic matrices, such as polypropylene (PP)[3,5–19] and polyethylene (PE),[2,4,20–27] which are the most frequently used polymers within the field of pulp fiber–reinforced thermoplastics. One of the main reasons is the limited stability of lignocellulosic fibers at temperatures exceeding 200°C. Therefore, little attention has been paid to the intrinsic properties of the fibers themselves. Second, pulp fibers available on the market emanate from large-scale pulping operations optimized for paper and cardboard applications. Neither the fiber source nor the pulping parameters are thus adapted to the use of these fibers as a reinforcement of thermoplastics. Paper strength is favored by the creation of large, strongly bonded surfaces between the fibers. This is achieved by refining the fibers to increase their wet flexibility, which improves fiber drape and network consolidation,[28] or in the case of mechanical pulps, by the mixing of long fibers and fines.[29] On the contrary, in composites, fiber bonding should be avoided because it prevents good fiber dispersion in the polymer matrix and is thus not desired. Furthermore, fibers should preferably be straight, stiff, strong, and of high aspect ratio to obtain good reinforcement.

*Present address: Nestlé Research Center Lausanne, Verschez-les-blanc, CH 1000 Lausanne, Switzerland.

Correspondence to: J.-A. Månson (jan-anders.manson@epfl.ch).

Journal of Applied Polymer Science, Vol. 92, 2132–2143 (2004)

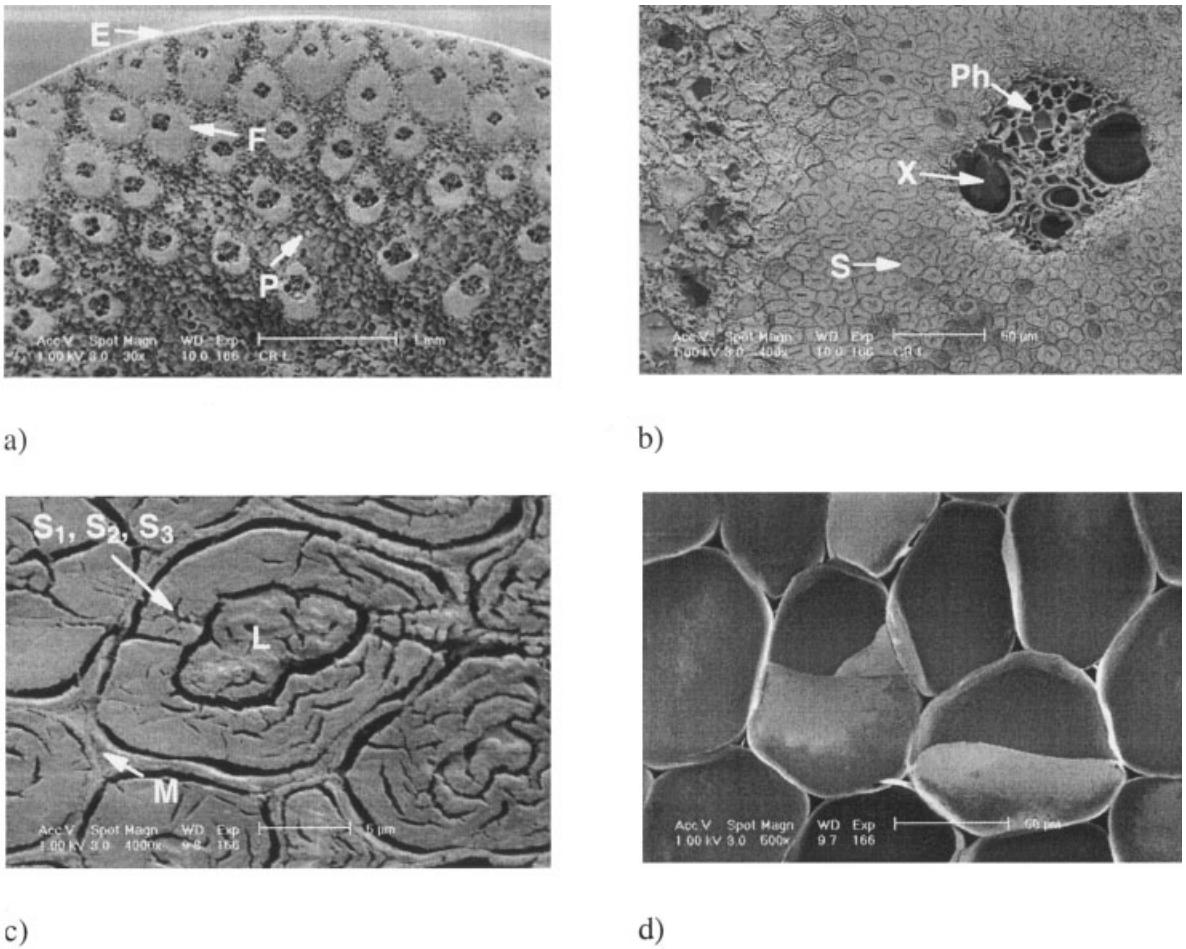

Figure 1 (a) China reed plant cross section showing fiber bundles (F) surrounded by parenchyma cells (P) and the protecting epidermis (E); (b) fiber bundle with central phloem (Ph) surrounded by sclerenchyma cells (S); (c) close-up of sclerenchyma cell where the central lumen (L), the S_1, S_2, and S_3 layers, and the middle lamella M can be distinguished; (d) homocellular axial parenchyma cells.

A further requirement is that the fibers withstand high temperatures during the time span of processing operations.

For the aforementioned reasons the raw material selected for this study was china reed (*Miscanthus x giganteus*), a fast-growing perennial C_4 plant with thick-walled fibers, which is likely to correspond to the requirements on straightness and stiffness for composite reinforcements. Although only one fiber source was investigated in this study, the reasoning and conclusions drawn here are valid for all fiber sources. The present study investigates the influence of alkali–methanol–anthraquinone (AMA) pulping conditions on the mechanical and thermal properties of *Miscanthus x giganteus* in view of an optimization of these properties for composite applications.

EXPERIMENTAL

Materials

The morphology of *Miscanthus* was investigated on a polished gold sputter–coated transverse stem section under a Philips XLF-30 scanning electron microscope (Philips, The Netherlands) at an acceleration voltage of 1 kV. Three main structural features can be distinguished in the plant cross section [Fig. 1(a)]. The epidermis (E), 8 vol %, is a thin silica-rich layer located at the exterior of the plant to protect it against external aggressions. Fiber bundles (F), 30 vol %, are visible as slightly oval structures with increasing size toward the epidermis. The fiber bundles toward the core of the plant contain about 50 fibers each, whereas the fiber bundles toward the surface can contain as many as 250 fibers. Honeycomb-like parenchyma cells (P), 62 vol %, dominate the core of the plant. Figure 1(b) shows the structure of the fiber bundles. The core consists of the xylem cells (X), conducting water from the roots to the leaves, and the phloem cells (Ph), conducting photosynthesis products in the opposite direction. The core is surrounded by sclerenchyma cells (S), which will be referred to as fibers in this report. The fibers have a central lumen (L) surrounded by the secondary wall, dominated by the S_2 layer, which is a thick layer of highly ordered cellulose mi-

crofibrils conferring stiffness to the fiber.[30] The fibers are cemented together by the middle lamella (M), which is primarily constituted by lignin [Fig. 1(c)]. Parenchyma cells are axial thin-walled cells mainly containing hemicellulose and lignin [Fig. 1(d)]. Mechanically, these cells serve as a foam core in an axisymmetric sandwich structure, accommodating shear, whereas the stiff outer layer of the plant accommodates compression and tension forces. As evident in Figure 1(c), the middle lamella constitutes a potential weak point in the structure of the fiber bundles. In addition to this, the hemicellulose-rich parenchyma has low mechanical properties and would not reinforce a polymer matrix to as high an extent as would individual fibers. Consequently, an optimized extraction process would permit extracting individual fibers while excluding middle walls and parenchyma.

Miscanthus x giganteus samples harvested in March 1999 and cut into chips approximately 0.5×2 cm^2 in size during harvesting were screened according to SCAN-CM 40 : 9 using a chip classifier with holes of 5.0 ± 0.3 mm diameter mounted on a shaking frame. The stroke was 120 mm and the frequency approximately 180 cycles/min. The chips were swelled in water at a consistency of 1 : 13 solid to liquid ratio (SL) at 4°C for 24 h before acid washing in aquatic H_2SO_4 at pH 3 at 1 : 20 SL and 60°C for 1 h to remove metal salts, which may reduce selectivity or even function as delignification inhibitors. After the acid wash, the chips were washed back to their initial pH value in water dispersion (five times at 1 : 20 SL) and dried to a moisture content below 8% to improve the impregnation of the chips by the pulping liquor. The pulping liquor was prepared by mixing dry 99.9% pure NaOH pellets with a previously mixed solution of demineralized water and methanol. Subsequently the china reed chips (11 g dry weight) were inserted into stainless-steel reactors together with anthraquinone crystals placed in the middle of the chip stack. After addition of the pulping liquor, the reactors were evacuated by vacuum and flushed with nitrogen three times to remove oxygen, which may intervene in the delignification process. Subsequently the reactors were carefully sealed and fixed on reactor holders mounted on a rotating axis, which was then plunged into an oil bath preheated to the desired pulping temperature. The rotating speed of the axis was 4 rpm. Once the predetermined reaction time came to an end the pulping process was stopped by cooling the reactors under running water. The black liquor resulting from the pulping stage was drained out of the reactors as far as possible and kept for analysis. The resulting pulps were washed with water six times at 1 : 40 SL to remove the residual black liquor absorbed by the pulp fibers. The pulp samples were stored overnight immersed in water to verify by color inspection whether the washing was satisfactory. In case it was not, the procedure was repeated.

TABLE I
Independent Variables for Pulping Experiments

Variable	Low conditions (−)	High conditions (+)
Soda (% odw)	15	30
Methanol (vol %)	10	40
Pulping time (min)	25	75
Pulping temperature (°C)	150	170

After washing, each pulp sample was defibrated in a propeller mixer (British Standard Pulp Evaluation Apparatus, Mavis Engineering Ltd., London, UK) at about 1 : 200 SL for 200 s at 3000 rpm. Already before this step visual inspection revealed that most of the pulp was already defibrated. The defibration time was thus kept to a minimum to avoid unnecessary fiber damage. The pulps were screened according to the procedure described in the next section to extract knots and impurities.

Factorial design for pulping analysis

Many experiments involve the study of the effects of two or more factors. In general factorial designs are most efficient for this type of experiment because they permit investigating the effect of all possible combinations of the levels of experimental factors.[31] In this study an unreplicated 2^4 factorial design was used to evaluate the effect of the four pulping factors (NaOH concentration, methanol concentration, pulping temperature, and pulping time) on the dependent properties (thermal stability, fiber strength, residual lignin content, viscosity, and screened yield). Table I shows the high and low conditions for each of the independent pulping variables. The solids to liquid ratio and the anthraquinone charge were kept constant at 1 : 4[32–34] and 0.1% on dry chip weight[33,35,36] for all pulping conditions. The setup for the experimental design is listed in Table II. Normal probability plots were used to compare the important effects and interactions involved in the experiments.

Thermogravimetric (TGA) measurements were performed to determine the thermal stability of the pulped fibers. The results were compared with the thermal stability of the as-delivered china reed and china reed having been submitted to a 2-h hot water extraction with subsequent washing to rid the sample of mineral salts. All investigated samples were dried under vacuum at 105°C for 4 h before analysis. The average sample weight was 7.5 ± 0.5 mg. Ground china reed particles were placed directly onto the sample tray, whereas in the case of pulped fibers three circular discs, 4 mm in diameter, were cut out of paper

TABLE II
Experimental Design Where Plus Signs (+) Denote High Conditions and Minus Signs (−) Represent Low Conditions as Described in Table I

Run no.	Methanol (M)	NaOH (S)	Time (T)	Temperature (C)
1	−	−	−	−
2	+	−	−	−
3	−	+	−	−
4	+	+	−	−
5	−	−	+	−
6	+	−	+	−
7	−	+	+	−
8	+	+	+	−
9	−	−	−	+
10	+	−	−	+
11	−	+	−	+
12	+	+	−	+
13	−	−	+	+
14	+	−	+	+
15	−	+	+	+
16	+	+	+	+

prepared from each batch. To eliminate water absorbed during transfer to the TGA sample chamber, the thermal cycle was initiated with an isotherm at 105°C for 5 min. The weight loss and derivative weight loss were then recorded as a function of time and temperature up to a temperature of 450°C at a heating rate of 20°C/min, under a nitrogen atmosphere. The onset of thermal degradation was defined as the point where 1% weight loss was observed. The experimental error in temperature was derived from the experimental curves based on the ±0.1% accuracy of the thermobalance.

Homogeneous isotropic sheets were produced from screened pulps according to ISO 5269. The produced sheets were stored overnight at 23°C and 50% relative humidity. Sheet grammage was calculated according to ISO 536. The fiber tensile strength was evaluated by means of zero-span tensile index according to ISO 15361-2000 (E) using rewet sheets of unbeaten fibers. Lignin content was determined in terms of Kappa number, by titration with potassium permanganate according to the standard test method ISO 302-1981 (ISO 1998). The Kappa number is directly proportional to the lignin content by a proportionality factor, which is proper to each plant species. A high Kappa number equals a high lignin content, and a Kappa number of one corresponds to 0.167% residual lignin. Because it was not necessary to determine the absolute value of the lignin content, the samples were compared based directly on the Kappa values.

Fiber production

Based on results from the small-scale pulping of the experimental design, two sets of pulping conditions were selected for upscaling. The upscaled pulping experiments were performed using 600 g of raw material for each batch. The 600 g of raw material were divided into two reactors each containing 300 g of material. The reactors were immersed in an oil bath similar to that used in small-scale pulping. Apart from generating material for further experiments these tests served to investigate the reproducibility of the factorial design on a larger scale. Because of the batch nature of the pulping, pulping conditions at the same temperature were selected. The pulped and drained chips were not washed manually as in the factorial experiments. Instead, they were placed in cylinders with a wire mesh bottom and kept overnight under sprinkling water to wash out residual pulping chemicals. The upscaled pulps were defibrated in a water jet defibrator equipped with a 3-mm screen followed by a Wennerberg 0.15-mm slit screen and dewatered in a centrifuge to 25% dry weight.

Fiber characterization methods

In addition to the analyses performed on the pulps generated from the experimental design, the size and shape of the upscaled pulps were analyzed in an STFI FiberMaster 2 analyzer (Lorentzen & Wettre, Kista, Sweden). Because only dry fiber dimensions are relevant to the use of pulp fibers as a reinforcement of thermoplastics, the data obtained from the FiberMaster measurements were corrected to take the degree of radial shrinkage from the wet state to the dry state into account, assuming that longitudinal fiber shrinkage is negligible.[30] The radial shrinkage was measured using an Olympus BHZ-UMA optical microscope (Olympus, Osaka, Japan) equipped with a hot stage. A suspension of fibers in demineralized water was placed on a microscopy glass. The fibers were allowed to absorb water for 5 min, after which micrographs of wet fibers were taken, as shown in Figure 2(a). The hot stage was then heated at 20°C/min to 105°C on which the water was evaporated. The fibers were allowed to dry 5 min from the moment when no visible water remained before another micrograph was acquired [Fig. 2(b)]. The radial shrinkage was subsequently calculated from 10 measurements on selected fibers dried once at room temperature and rewet, drying conditions that were identical to those of the fibers analyzed in the STFI FiberMaster measurements. It is known that the swelling of fibers is reduced considerably after the first drying and that as drying conditions become more severe, the swelling is reduced further.[37,38] The radial fiber shrinkage attributed to drying to 105°C was found to be 29 ± 1%. The diameter values obtained by the FiberMaster measurements were corrected with these values.

The longitudinal tensile strength of the upscaled fibers was derived from the results of the zero-span

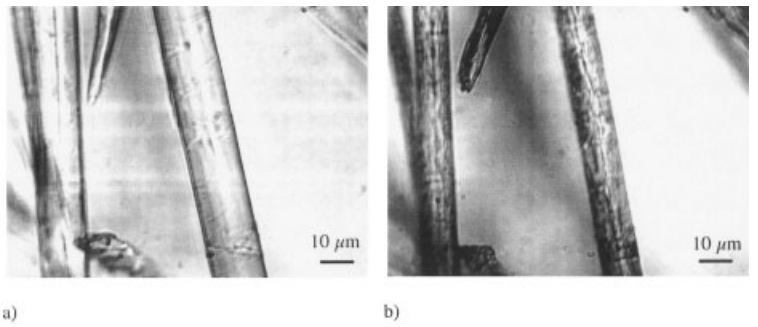

Figure 2 Micrographs showing (a) a wet china reed pulp fiber and (b) a dry china reed pulp fiber.

tests, taking fiber orientation and residual span length into account as detailed in a later section. These values were compared to the tensile strength of rectangular sections cut out from the surface layer of a china reed stem measured using a UTS tensile tester at a crosshead speed of 1 mm/min. The area of the cross sections varied between 0.5 and 1 mm^2 and the tensile strength measurements were corrected assuming fiber bundles to be the only load-carrying component of the cross section. Because the mechanical properties of brittle fibers were size-dependent as a result of the presence of defects on the surface and in the bulk of the fiber,[39–43] three gauge lengths (15.5, 20, and 43.8 mm) were tested to determine the relation between gauge length and mechanical properties. The test samples were glued with cyanoacrylate adhesive into a slot in flat aluminum sample holders to ensure that the samples were well aligned with the direction of the applied force. Because the test specimen cross section is constituted only partially by fiber bundles, postmortem cross sections were cut perpendicularly to the loading axis in the vicinity of the rupture surface, carefully polished, and examined by optical microscopy to determine the effective load-bearing cross section, assuming that parenchyma cells carry no tensile load.

The intrinsic density of samples from upscaled pulping was measured by helium pycnometry on a Micrometrics AccuPyc 1330 (Creil, France). This method consists in measuring the displaced gas volume by a sample of known weight. The density of the sample is calculated as sample weight over displaced gas volume. The sample, dried 12 h in vacuum at 105°C before testing, was introduced into the sample chamber, which was then flushed several times with gas before the actual measurements were made. The sample weight was in all cases 0.6 g. Ten consecutive measurements were made per sample.

RESULTS AND DISCUSSION

Delignification

The normal probability plot of factor effects on Kappa number is shown in Figure 3. The factors temperature (C), pulping time (T), soda concentration (S), and the interaction between temperature and pulping time (TC) deviate significantly from the line, and should thus be considered as significant effects on Kappa number. All the significant main effects (C, T, and S) are negative, meaning that running all these factors at a lower level would maximize the Kappa number (i.e., reduce the delignification efficiency). Methanol has been shown to enhance delignification as well as selectivity for several systems.[33,34,44,45] According to the normal probability plot, however, methanol does not have a significant effect on delignification for this specific reed plant. Similar observations were reported by Colodette et al. for methanol–kraft pulping of eucalyptus.[46] In general, the delignification efficiency was found to be very high for the investigated pulping conditions, which is in agreement with observations made elsewhere for this process.[47]

Thermal stability

The temperature of 1% weight loss (T1%) of the as-delivered china reed was found to be equal to 203 ± 4°C, which is in the range of processing temperatures of common commodity thermoplastics such as polyethylene and polypropylene, thus involving a risk of thermal degradation during processing. Hot-water

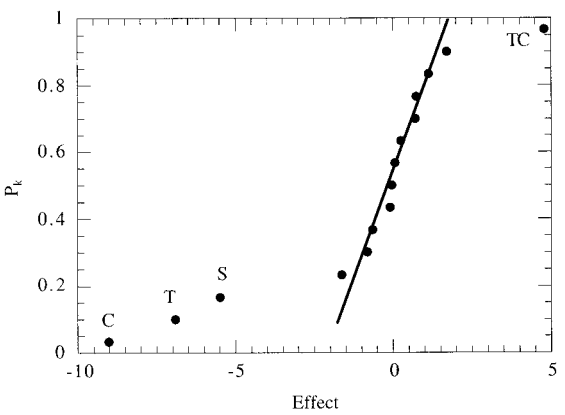

Figure 3 Normal probability plot of estimates of the effects of factors and interaction on the Kappa number.

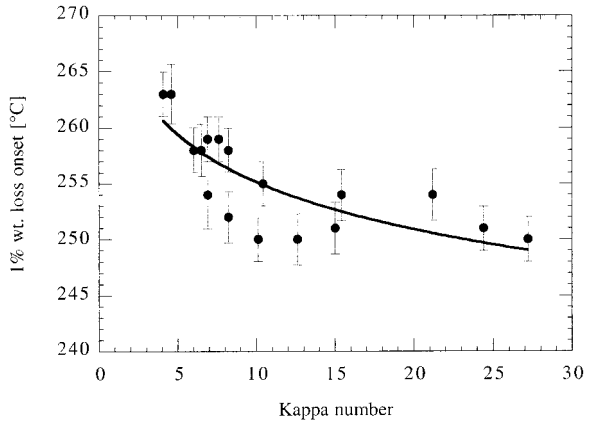

Figure 4 Thermal stability as a function of delignification measured by the Kappa number. The line is a guide for the eye.

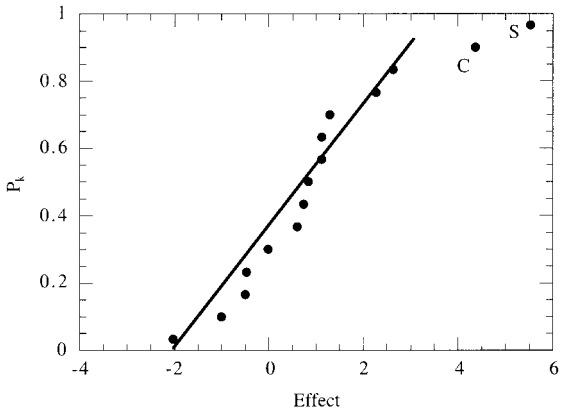

Figure 5 Normal probability plot of estimates of the effects of factors and interactions on thermal stability measured by thermogravimetry.

extraction increased the thermal stability significantly to 251 ± 3°C, which is sufficient for frequently used processing times and temperatures. This demonstrates the important catalytic effect of mineral salts on thermal degradation of wood polymers observed by Szabó et al.[48] In the absence of mineral salts, the thermal stability of any given pulp is determined by its composition in terms of cellulose, hemicellulose, and lignin.[48–51] As shown in Figure 4, where T1% is represented as a function of Kappa number, within the investigated range of pulping parameters, the thermal stability of the fibers is only marginally improved by pulping.

The thermal stability of lignocellulosic materials is a function of chemical composition. The Kappa number is representative of the extent of delignification as well as indirectly of the removal of hemicellulose in a given processing sequence. There is a clear monotonous trend of increasing thermal resistance with reduced Kappa number, related to the removal of lignin, and hemicellulose, which is the least stable wood polymer.[49] The chemical composition analysis revealed that the AMA process was particularly efficient in removing xylane and lignin from the fiber structure. It is thus favorable to remove as much hemicellulose as possible, to optimize the thermal resistance of the fibers. Nevertheless, the range of observed thermal stability should not be a limiting factor for the typical processing temperatures of the commodity thermoplastics most frequently used with pulp fiber reinforcement. Furthermore, it is evident on the normal probability plot presented in Figure 5 that only the factors soda quantity (S) and pulping temperature (C) present a significant effect with positive values. Increasing these factors will thus improve thermal stability.

Zero-span tensile index rewetted

The normal probability plot of effects for the zero-span tensile index in Figure 6 reveals no statistically significant effects within the range of experimental parameters investigated in this study. Unbeaten china reed pulp fibers exhibit zero-span tensile index values in the range of 148–187 Nm/g, as shown against Kappa number in Figure 7. These values are considerably higher than strength values of 100 Nm/g obtained elsewhere for ethanol–alkali pulped reed canary grass,[32] a similar species in terms of origin and shape to *Miscanthus x giganteus*.[52] The highest zero-span values were observed for pulping conditions 9 and 13 (~ 187 Nm/g) with Kappa numbers in the vicinity of 10. Pulping to lower Kappa numbers results in a loss of strength. However, as evident in the figure, the discrepancy in zero-span values between samples of similar Kappa number is considerable, especially at high Kappa numbers. Page et al.[53] suggested that for nondegrading pulping processes, fiber strength is proportional to α-cellulose content over a wide yield

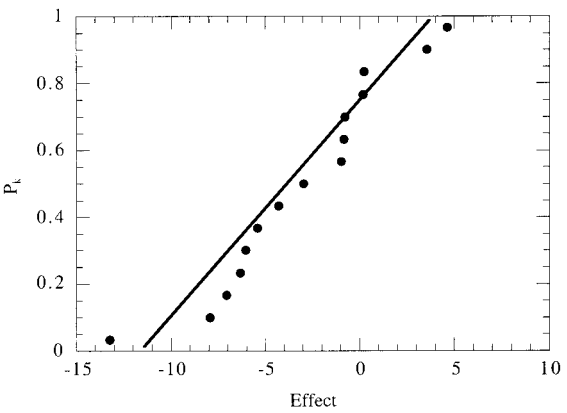

Figure 6 Normal probability plot for the effects of factors and interactions on zero-span tensile index.

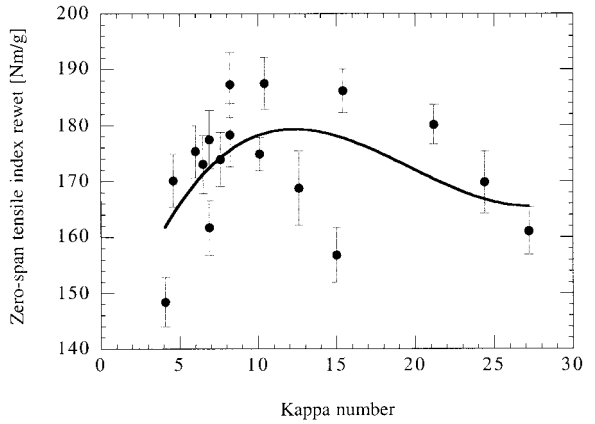

Figure 7 Zero-span tensile index rewet as a function of Kappa number. The line is a guide for the eye.

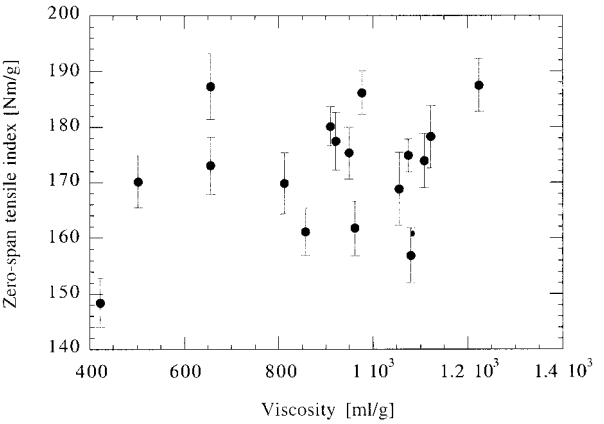

Figure 8 Zero-span tensile index rewet as a function of pulp viscosity.

range up to a cellulose content of about 80%. Pulping beyond this point would then remove the hemicellulose and lignin constituents, directly contributing to stress transfer between the cellulose fibrils in the S_2 layer, with a resulting decrease in mechanical properties. This hypothesis partially explains the behavior observed here.

Pulp viscosity is frequently used as an indirect measure of pulp strength. The zero-span tensile index is represented against pulp viscosity in Figure 8. The lowest zero-span index is indeed observed for the pulp with the lowest intrinsic viscosity (423 mL/g). Molin and Lennholm[54] observed consistent zero-span strength down to a cellulose intrinsic viscosity of 500 mL/g after which a rapid strength decrease was observed, which is in agreement with the present observation. In the present study, however, the zero-span tensile index is far from consistent above this viscosity value. Seth and Chan[55] have questioned the validity of interpreting high viscosity values with high values of pulp strength, based on experimental results showing variations of only $\pm 10\%$ of zero-span tensile strength for pulp viscosities ranging from 14 to 28 mPa s^{-1}. The validity of this argument is supported by the fact that the second lowest zero-span tensile index is observed for a pulp with a viscosity as high as 1087 mL/g. The high scatter in zero-span values at higher viscosity suggests that above a certain threshold viscosity, fiber mechanical properties are governed by parameters other than merely viscosity. Agarwal and Gustafson[56] noted that primary peeling, or end-initiated depolymerization, had a positive effect on mechanical properties, whereas secondary peeling, or chain scission, had a negative effect on fiber strength. The reason for this complex behavior must thus be sought in the contributions of the wood polymers to strength. Removal of hemicellulose and lignin accompanied by the removal of low molecular weight cellulose improves the mechanical properties of the fibers while also improving the thermal stability, up to a certain point. Further delignification will degrade the cellulose and remove the fractions of lignin and hemicellulose that contribute positively to fiber strength.[56]

The Kappa number was the only measure of chemical composition used in this study. Assuming the Kappa number to be inversely proportional to cellulose content is hazardous, given that the efficiency of hemicellulose removal relative to that of delignification may vary with varying pulping conditions. A thorough analysis of the composition of the samples in terms of cellulose, hemicellulose, and lignin content coupled with morphological studies would undoubtedly shed additional light on this issue and permit drawing more stringent conclusions, although such an investigation is beyond the scope of this study.

Selection of pulping conditions for upscaled pulping

The goal of the pulping investigation was to optimize the thermal stability and mechanical properties of the

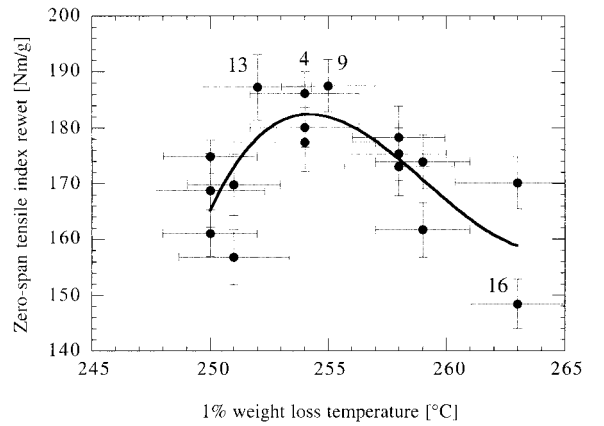

Figure 9 Zero-span tensile index rewet as a function of thermal stability. The line is a guide for the eye.

TABLE III
Pulping Parameters for Upscaled Pulping

Batch	Methanol (vol %)	Soda (% odw)	Pulping time (min)	Pulping temperature (°C)
13	10	15	75	170
16	40	30	75	170

fibers in view of their use as reinforcement in thermoplastics. Because the thermal stability increases steadily with decreasing Kappa number, whereas the zero-span tensile index goes through a maximum, a trade-off between the two properties has to be accepted. This trade-off is illustrated in Figure 9, where zero-span tensile index is represented as a function of thermal stability.

Nevertheless, in the context of polymer processing a thermal stability of 250°C is judged satisfactory, and the mechanical properties were retained as the sole selection criterion. Three experimental conditions distinguished themselves from the others in terms of zero-span tensile strength: batches 4, 9, and 13, which are indicated in the figure. Within experimental error both their thermal stability and strength are equal. Based on absolute values the conditions used for batch 9 led to the highest zero-span tensile strength (187.5 Nm/g) for a 1% weight loss onset temperature of 255°C. The experimental conditions for this batch corresponded to low levels of all pulping parameters but temperature, which is also interesting from an environmental point of view. For composite processing reasons it was interesting to retain pulp fibers representing high and low mechanical properties. To avoid interrupting the batch pulping process it was thus decided to retain pulping conditions 13 and 16, representing pulps of high strength–intermediate thermal stability, and low strength–high thermal stability, respectively, for upscaled pulping, given that they have identical pulping temperature and time. The used pulping conditions are shown in Table III.

Upscaled pulping

Table IV shows a comparison of the upscaled pulping analyses (suffix U) to the values of the experimental design (no suffix). The change of scale (30 times larger) gave slight differences in the outcome of the pulping. The rate of delignification was found to be lower for the large experiments compared to the others. The same holds true for the fiber strength. Nevertheless, the order of the results between the different conditions was respected in all cases.

The reason for the differences between the experimental design pulping and the upscaled pulping is first the dispersion of the anthraquinone within the pulping liquor. As indicated earlier anthraquinone is not soluble in the pulping liquid at room temperature. The anthraquinone was therefore placed in the center of the chip stack as was done for the experimental design pulping. However, because of the difference in scale of the reactors the anthraquinone was less homogeneously distributed throughout the bulk of the sample, thus reducing the overall delignification rate. In addition, because of the difference in scale, heating was also slower because of lower heat transfer efficiency in the large reactors used for upscaled pulping.

Fiber size distribution analysis

The fiber size and aspect ratio distributions of the analyzed samples are displayed in Figure 10. The fiber length distributions are similar to those of straw fibers[57] with a number-average value of 0.552 and 0.491 mm for batches 13 and 16, respectively. The fiber diameter was found to be quite uniform, with average values of about 13 μm, giving the fibers a number-average aspect ratio of about 40, similar to that of short glass fibers for injection molding. The average dimensions and shape factors of the fibers are reported in Table V. The straightness of the fibers is high with a shape factor f_s as high as 95%, which is characteristic for hardwood pulps[58] compared to values of 80%, which are common for commercial bleached softwood kraft pulps.[59] The straightness of the fibers is an advantage from a reinforcement point of view.

Mechanical properties

The mechanical properties in terms of Young's modulus and strength as a function of gauge length are

TABLE IV
Comparison of Results of Upscaled Pulps with Pulps of the Experimental Design

	13U	13	16U	16
pH Black liquor	11.34	11.38	11.86	11.96
Residual alkali (mol/L)	0.042	0.043	0.523	0.587
Kappa number	12.5	8.2	5.8	4.1
Viscosity (mL/g)	1200	1108	570	423
Zero-span tensile index rewet (Nm/g)	173.2	187.3	138.7	148.2
Intrinsic density (g/cm^3)	1.5306 ± 0.0013		1.5436 ± 0.0013	

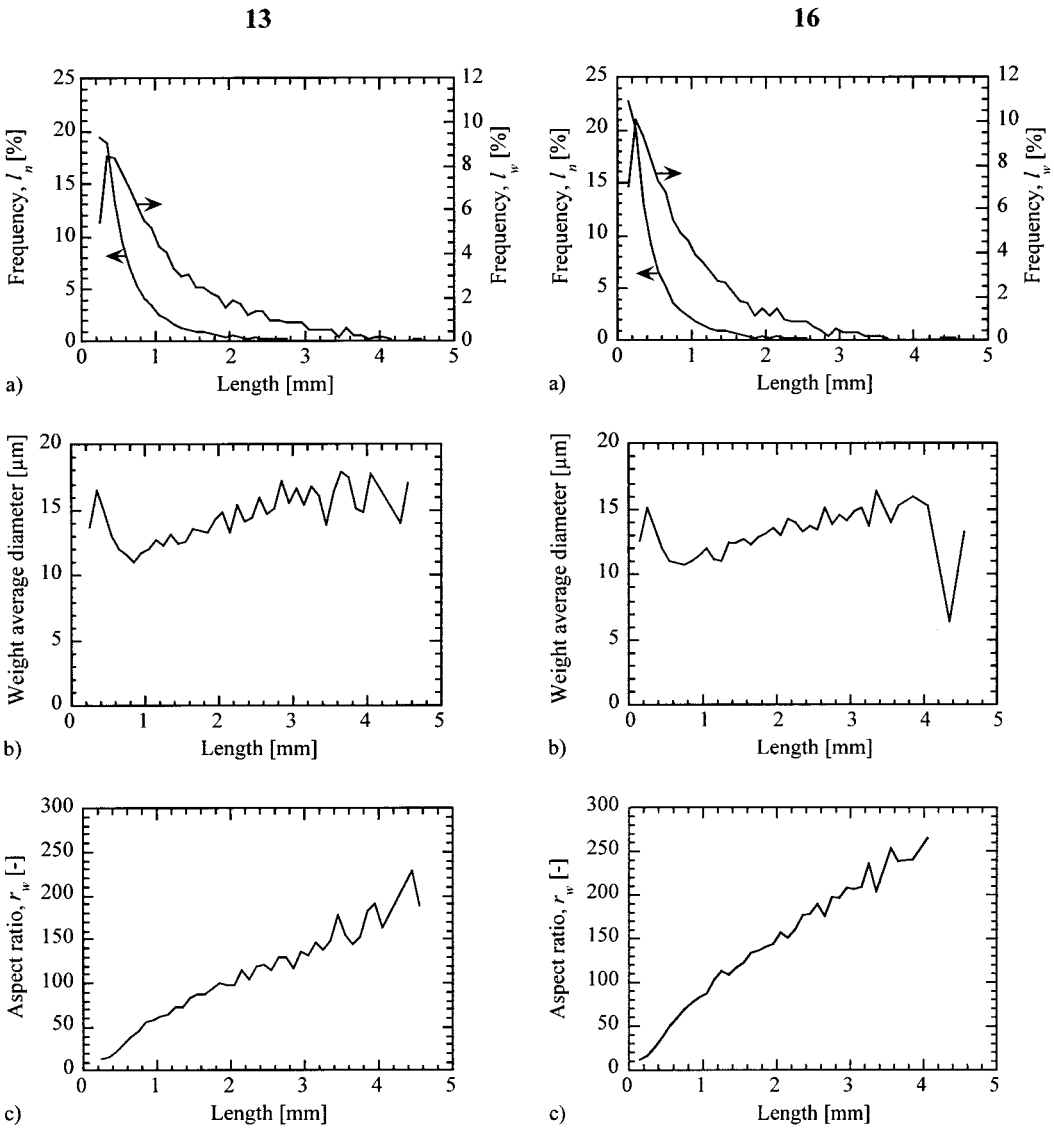

Figure 10 Size distribution of upscaled pulps: (a) number- and weight-average length distribution; (b) corrected weight-average diameter distribution; (c) aspect ratio distribution.

represented in Figure 11(a) and (b). Assuming as a first approximation that (1) both Young's modulus and tensile strength are linearly proportional to the gauge length as reported in previous studies,[39–41,43,60] (2) no change in failure mechanisms occurs at short gauge lengths, and (3) the material is not strain rate dependent within the range of strain rates (4×10^{-4} to 1×10^{-3} s^{-1}) used in the experiment, and using the number-average length of the pulped fibers, the extrapolated Young's modulus and tensile strength—taking into account fiber bundles as the only load-carrying component—were found to be equal to 59.5 ± 0.4 GPa and 913 ± 79 MPa, respectively. These values are expected to be representative of the stiffness and strength of pulped fibers.

TABLE V
Size and Shape Averages for the Pulped Samples

Sample	l_n (mm)	l_w (mm)	d_h (mm)	d_w (mm)	r_n	r_w	f_s (%)
13	0.552	1.086	13.45	13.70	40.3	80.7	95.1
16	0.491	0.962	12.46	12.67	38.7	77.2	94.3

The zero-span tensile index as measured on pulp sheets represents the strength of a randomly oriented two-dimensional (2D) structure of fibers. The following analysis was developed to calculate the longitudinal tensile strength of individual pulp fibers from measured zero-span values, required for modeling of composite tensile strength. Van den Akker introduced the original zero-span equation[61]

$$Z = N\Phi F_S \tag{1}$$

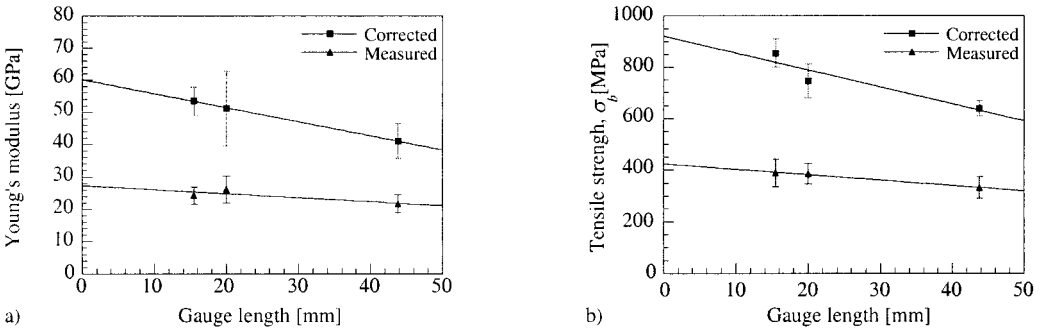

Figure 11 Measured and parenchyma-corrected Young's modulus (a) and tensile strength (b) of stem samples as a function of gauge length. The lines are the results of linear regression analysis.

where Z is the paper zero-span failure load, Φ is a factor that accounts for fiber orientation, F_S is the unknown average specific force at failure of fibers in the tested sheet, and N is the number of load-carrying fibers. For a randomly oriented 2D network, Φ is equal to 3/8.[59] This model assumes that all fibers in the cross section transmit load during the test and that the tested span is of zero length. However, a finite span necessarily exists when failure occurs, which indicates the existence of a greater span over which microslippage and stretch occur. Boucai[62] deduced the following probability function, which governs the fraction of fibers (Ψ) in a random aggregate, which will cross both of two adjacent clamping lines relative to the number that will cross either of the lines alone:

$$\Psi = \frac{2}{\pi}\left[\left(\frac{\pi}{2} - \sin^{-1}\left(\frac{\partial}{l_n}\right)\right) - \frac{\partial}{9l_n}\sqrt{1 - \frac{\partial^2}{l_n^2}}\left(7 + \frac{2\partial^2}{l_n^2}\right)\right] \quad (2)$$

where ∂ is the residual span and l_n is the number-average fiber length. Taking this factor into account, eq. (1) becomes

$$Z = \Psi N \Phi F_S \quad (3)$$

Although the above expression is useful to generate information on the force required to break a fiber it does not allow calculation of the tensile stress in the fiber cross section at the moment of failure unless the exact degree of hollowness of the fibers is known. Knowing the absolute density of the fibers in the tested sheets and knowing the grammage of the same, the tensile stress at break, σ_s^b, of the load-carrying section of fibers in the paper can be calculated as

$$\sigma_s^b = \frac{Z_{rw}G}{G/\rho_f^i} = Z_{rw}\rho_f^i \quad (4)$$

where the zero-span tensile index Z_{rw} is equal to Z/cG (Nm/g), G is the grammage of the tested sheets (g/m^2), c the width of the test coupon, and ρ_f^i is the intrinsic density of the fibers (g/m^3) as measured by helium pycnometry. By taking the random 2D fiber distribution into account, the longitudinal tensile strength of the fibers σ_f^l thus becomes

$$\sigma_f^l = \frac{Z_{rw}\rho_f^i}{\Psi\Phi} \quad (5)$$

where Φ takes the value 3/8 for the random 2D case and Ψ is given by eq. (2). Using the number-average fiber length of the fibers, as analyzed in the previous section, the tensile strength of the fibers evolves with the residual span length ∂ according to Figure 12 and, assuming a residual span of 0.1 mm,[63] eq. (5) yields a longitudinal tensile fiber strength of 889 and 743 MPa for fibers 13 and 16, respectively. As seen in the figure the assumption of residual span length is quite conservative and may underestimate the real strength of the fibers. Nevertheless, the obtained strength values are of the same order of magnitude as those obtained from the tensile tests on stem sections.

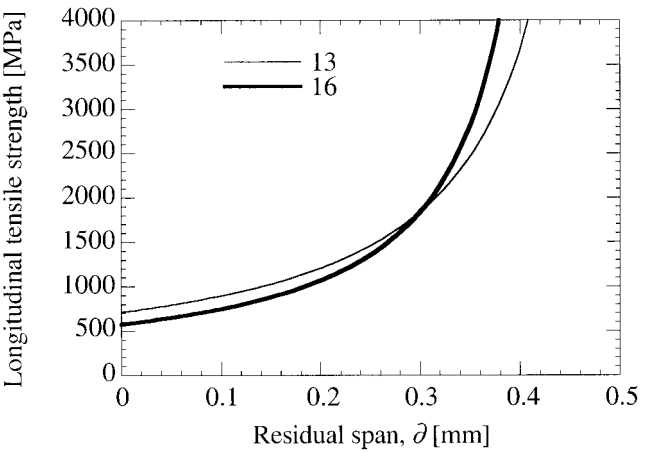

Figure 12 Calculated longitudinal strength of fibers emanating from upscaled pulping according to conditions 13 and 16 as a function of assumed residual span length.

TABLE VI
Comparison of the Specific Properties with Respect to Cost and Density of the Generated Fibers and with Glass Fibers[a]

Fiber type	Cost, c ($/kg)	Density, ρ (kg/m^3)	Young's modulus, E (MPa)	Tensile strength, σ (MPa)	E/ρ (GPa m^{-3} kg^{-1})	σ/ρ (GPa m^{-3} kg^{-1})	$E/\rho c$ (GPa m^{-3} \$$^{-1}$)	$\sigma/\rho c$ (MPa m^{-3} \$$^{-1}$)
GF	2	2560	76,000	1400–2500	29.7	0.55–0.98	14.8	270–490
13	0.7	1531	59,900	889	39.1	0.58	55.9	820
16	0.7	1544	59,900	743	38.8	0.48	55.4	690

[a] Refs. 64–66.

The tensile properties of these fibers are quite low compared to those of glass fibers on an absolute scale. A fair comparison should take into account the fact that pulp fibers have lower cost and lower density. Table VI compares the specific stiffness and strength with respect to cost and density of the pulp fibers generated in this study to those of glass fibers. Pulping yields single fibers of straightness as high as 95% with specific strength and stiffness with respect to cost and density, which are remarkably higher than those of glass fiber alternatives. If this advantage can be conserved throughout the composite processing operations the generated materials will be highly competitive to short glass fiber–reinforced composites in load-bearing applications.

CONCLUSIONS

The objective of the pulping study was to determine the key pulping parameters that directly influence the mechanical and thermal properties of alkaline–methanol–anthraquinone pulped china reed fibers. An unreplicated 2^4 factorial design was used for the optimization of mechanical properties and thermal stability. The optimum pulping conditions based on strength and thermal resistance measurements were the following:

- Methanol concentration: 10 vol %
- Alkali concentration: 15 wt % on dry chip weight
- Pulping time: 25 min
- Pulping temperature: 170°C

These parameters correspond to a zero-span tensile index of 187.5 Nm/g and a 1% weight loss onset temperature of 255°C. The major effects contributing to improved thermal stability of pulp fibers were found to be soda quantity and temperature. It was found that thermal stability increased monotonously with decreasing lignin content within the investigated range. The zero-span tensile index was found to have a maximum at Kappa numbers around 10. It is thus possible to improve simultaneously the thermal stability and the mechanical properties of the fibers up to this value. In addition to the experimental design, upscaled pulping experiments were made for selected samples. For the same experimental conditions, a decrease of about 7% was noticed for the zero-span values compared with those of the small-scale experiments, a probable result of uneven distribution of anthraquinone in the bulk of the chips, which may be avoided by using soluble or liquid anthraquinone to achieve a better dispersion.

A model was developed to calculate the longitudinal tensile fiber strength from the zero-span tensile index, taking into account fiber orientation and the effect of a finite residual span. Assuming a residual span of 0.1 mm, this model gives strength values of the order of 800 MPa. The Young's modulus of the fibers was found to be equal to about 59 GPa, from extrapolation of tensile data obtained on stem sections at various gauge lengths, to the number-average fiber length. The corresponding specific strength and stiffness, with respect to cost and density, are remarkably higher than those of glass fibers. Moreover, because they are characterized with straightness as high as 95%, pulp fibers are therefore interesting low-weight and low-cost alternatives to short glass fibers.

The authors gratefully acknowledge Genossenschaft Biomasse Technologie, Switzerland, for supplying the raw material used for this study; Ulrika Molin (Department of Pulp and Paper Chemistry and Technology, KTH, Sweden), for assistance in upscaled pulping experiments; and the staff at The Centre Interfacultaire de Microscopie Electronique (CIME-EPFL), for technical assistance in scanning electron microscopy.

References

1. Bledzki, A. K.; Gassan, J. Prog Polym Sci 1999, 24, 221.
2. Maskavs, M.; Kalnins, M.; Reihmane, S. In: Composites on the Base of Thermoplastic Polymers and Disperse Wood Waste, Proceedings of The Polymer Processing Society, Europe/Africa Meeting; The Polymer Processing Society: Gothenburg, Sweden, 1997.
3. Kazayawoko, M.; Balatinecz, J. J.; Woodhams, R. T. Law, S. Int J Polym Mater 1997, 37, 237.
4. Dong, S.; Sapieha, S.; Schreiber, H. P. Polym Eng Sci 1993, 33, 343.
5. Balatinecz, J. J.; Park, B.-D. J Thermoplast Compos Mater 1997, 10, 476.

6. Felix, J. M.; Gatenholm, P.; Schreiber, H. P. J Appl Polym Sci 1994, 51, 285.
7. Garkhail, S. K.; Heijenrath, R. W. H.; Peijs, T. Appl Compos Mater 2000, 7, 351.
8. Karnani, R.; Krishnan, M.; Narayan, R. Polym Eng Sci 1997, 37, 476.
9. Lu, M.; Collier, J. R.; Collier, B. J. In: Improving Mechanical Properties of Polypropylene–Wood Fiber Composites by Compounding and In-line Maleation, Proceedings of ANTEC 1995, Brookfield, CT.
10. Maldas, D.; Kokta, B. V. J Adhes Sci Technol 1994, 8, 1439.
11. Maldas, D.; Kokta, B. V. Int J Polym Mater 1994, 27, 77.
12. Maldas, D.; Kokta, B. V. J Thermoplast Compos Mater 1995, 8, 421.
13. Raj, R. G.; Kokta, B. V. J Appl Polym Sci 1989, 38, 1987.
14. Sain, M. M.; Kokta, B. V. J Appl Polym Sci 1993, 48, 2181.
15. Sain, M. M.; Kokta, B. V. J Adhes Sci Technol 1993, 7, 743.
16. Sain, M. M.; Kokta, B. V.; Maldas, D. J Adhes Sci Technol 1993, 7, 49.
17. Sain, M. M.; Kokta, B. V. Polym Plast Technol Eng 1994, 33, 89.
18. Sain, M. M.; Kokta, B. V. J Reinforced Plast Compos 1994, 13, 38.
19. Schneider, J. P.; Myers, G. E.; Clemons, C. M.; English, B. W. Eng Plast 1995, 8, 207.
20. Hedenberg, P.; Gatenholm, P. J Appl Polym Sci 1996, 60, 2377.
21. Liao, B.; Huang, Y.; Cong, G. J Appl Polym Sci 1997, 66, 1561.
22. Maldas, D.; Kokta, B. V. J Reinforced Plast Compos 1995, 14, 458.
23. Oksman, K. Wood Sci Technol 1996, 30, 197.
24. Park, B.-D.; Balatinecz, J. J. Int J Polym Mater 1997, 37, 133.
25. Raj, R. G.; Kokta, B. V.; Daneault, C. A. J Appl Polym Sci 1990, 40, 645.
26. Raj, R. G.; Kokta, B. V. Polym Eng Sci 1991, 31, 1358.
27. Yam, K. L.; Gogoi, B. K.; Lai, C. C.; Selke, S. E. Polym Eng Sci 1990, 30, 693.
28. Biermann, C. J. In: Refining and Pulp Characterization, Handbook of Pulp and Papermaking; Academic Press: London, 1996; p. 137.
29. Hartler, N.; Teder, A. Cellulosateknik, Vol. 2; Institutionen för Pappers- och Massateknik (KTH): Stockholm, 1997.
30. Biermann, C. J. Handbook of Pulp and Papermaking; Academic Press: London, 1996.
31. Montgomery, D. C. Design and Analysis of Experiments, 5th ed.; Wiley: New York, 2001.
32. Håkansson, H. Ethanol Pulping of Reed Canary Grass; Department of Forest Products and Chemical Engineering, Chalmers University of Technology: Gothenburg, 1995.
33. Neumann, N.; Kordsachia, O.; Patt, R. Papier 1997, 51, 573.
34. Norman, E.; Lindgren, T.; Edlund, U.; Teder, A. Holzforschung 1997, 51, 142.
35. Fleming, B. I.; Kubes, G. J.; MacLeod, J. M.; Bolker, H. I. TAPPI J 1978, 61, 43.
36. Puthson, P.; Kordachia, O.; Odermatt, J.; Zimmermann, M.; Patt, R. Holzforschung 1997, 51, 257.
37. Jayme, G.; Büttel, H. Papier 1966, 20, 357.
38. Lundberg, R.; de Ruvo, A. Sv Papperst 1978, 81, 355.
39. Kulkarni, A. G.; Satyanarayana, K. G.; Sukumaran, K.; Rohatgi, P. K. J Mater Sci 1981, 16, 905.
40. Kulkarni, A. G.; Satyanarayana, K. G.; Rohatgi, P. K.; Vijayan, K. J Mater Sci 1983, 18, 2290.
41. Mukherjee, P. S.; Satyanarayana, K. G. J Mater Sci 1984, 19, 3925.
42. Mukherjee, P. S.; Satyanarayana, K. G. J Mater Sci 1986, 21, 4162.
43. Satyanarayana, K. G.; Ravikumar, K. K.; Sukumaran, K.; Mukherjee, P. S.; Pillai, S. G. K.; Kulkarni, A. G. J Mater Sci 1986, 21, 57.
44. Norman, E.; Olm, L.; Teder, A. TAPPI J 1993, 76, 125.
45. Ray, A. K.; Mohanty, B.; Garceau, J. J. In: Methanol Based Organosolv Pulping of Wheat Straw of Indian Origin, Proceedings of the 1993 Pulping Conference; TAPPI Press: Atlanta, GA, 1993.
46. Colodette, J. L.; Carneiro, C. J. G.; Miranda, J. F.; Campos, A. S. In: Effect of Methanol in Kraft Pulping and Oxygen Bleaching of Eucalyptus, Proceedings of the VI Latinamerican Congress on Pulp and Paper, Torremolinos, Spain, 1992.
47. Zenaku, A. In: Alkali Alcohol Anthraquinone Pulping, Proceedings of the 7th ISWP China Paper Conference, 1993, Beijing; TAPPI Press: Atlanta, GA, 1993.
48. Szabó, P.; Varhegyi, G.; Till, F.; Faix, O. J Anal Appl Pyrol 1996, 36, 179.
49. Di Blasi, C. J Anal Appl Pyrol 1997, 42, 73.
50. Rajeswara Rao, T.; Sharma, A. Energy 1998, 23, 973.
51. Tamaru, K. Bull Chem Soc Jpn 1951, 24, 164.
52. Wisur, H.; Sjöberg, L.-A.; Ahlgren, P. Ind Crops Prod 1993, 2, 39.
53. Page, D. H.; Seth, R. S.; El-Hosseiny, F. In: Strength and Chemical Composition of Wood Pulp Fibers, Transactions of the Eighth Fundamental Research Symposium; Papermaking Raw Materials: Their Interaction with the Production Process and Their Effect on Paper Properties; Mechanical Engineering Publications: Oxford, UK, 1985.
54. Molin, U.; Lennholm. H. In: Influence of Molecular Weight on Mechanical Properties of Pulp Fibers, Proceedings of the 54th APPITA Annual Conference, Melbourne; APPITA: Australia, 2000.
55. Seth, R. S.; Chan, B. K. TAPPI J 1999, 82, 115.
56. Agarwal, N.; Gustafson, R. TAPPI J 1995, 78, 97.
57. Hartler, N.; Teder, A. Cellulosateknik, Vol. 1; Institutionen för Pappers- och Massateknik (KTH): Stockholm, 1995.
58. Robertson, G.; Olson, J.; Allen, P.; Chan, B.; Seth, R. TAPPI J 1999, 82, 10.
59. Seth, R. S. In: Zero-Span Tensile Strength of Papermaking Fibers, Proceedings of the 85th Annual PAPTAC Meeting, 1999; Preprints A161–A173.
60. Mukherjee, P. S.; Satyanarayana, K. G. J Mater Sci 1986, 21, 51.
61. Van der Akker, J. A.; Lathrop, A. L.; Voelker, M. L.; Dearth, L. R. TAPPI J 1958, 41, 416.
62. Boucai, E. Pulp Paper Mag Can 1971, 72, 73.
63. Cowan, W. F. Fiber Quality Testing: Theory and Practice (HRC 34); Pulmac Instruments International: Montpelier, VT, 1991.
64. Bürger, H.; Koine, A.; Maron, R.; Mieck, K.-P. Int Polym Sci Technol 1995, 22, 25.
65. Hull, D. An Introduction to Composite Materials, Cambridge Solid State Science Series; Cambridge Univ. Press: Cambridge, UK, 1981.
66. Rytkonen, A. Paperinfor: Pulp Price Forecast 2nd Quarter 2001; Paperinfo Oy: Helsinki, 2001.